Article

Understanding the Regioselectivity in the Oxidative Condensation of Catechins Using Pyrogallol-Type Model Compounds

Yuto Ochiai, Sayumi Hirose, and Emiko Yanase

J. Org. Chem., **Just Accepted Manuscript** • DOI: 10.1021/acs.joc.0c01612 • Publication Date (Web): 03 Sep 2020

Understanding the Regioselectivity in the Oxidative Condensation of Catechins Using Pyrogallol-Type Model Compounds

*Yuto Ochiai, Sayumi Hirose, and Emiko Yanase**

Faculty of Applied Biological Sciences, Gifu University, 1-1 Yanagido, Gifu 501-1193, Japan

ABSTRACT

Catechins are found in many foods, including tea. These compounds are bioactive. Previous studies have shown that catechins form dimers on oxidation, and there seem to be distinct regioselective effects. However, the dimerization mechanism and regioselectivity are not well understood. Therefore, we investigated the oxidation of four pyrogallol-type model compounds of epigallocatechin (EGC) having various substituents with 1 eq copper chloride and 30% dioxane in water. Compounds having 2C-2C or 2C-4C bonds in the B-ring were obtained in different product ratios. Comparison of the oxidation rates of each compound revealed that the model compounds having an oxygen

atom corresponding to the 1-position of the C-ring of EGC underwent slow oxidation. In addition, using density functional theory calculations, we found that the highest occupied molecular orbital energies of these compounds were higher than those of the others. Further, the 2C-2C-bonded oxidation product having an A-ring and an oxygen atom at the C-ring 1-position was confirmed to have the highest thermodynamic stability. From these results, it is suggested that the regioselective condensation reaction of the catechin B-ring is related to interactions between the A-rings, as indicated by earlier studies, and the presence of oxygen at the 1-position of the C-ring in EGC.

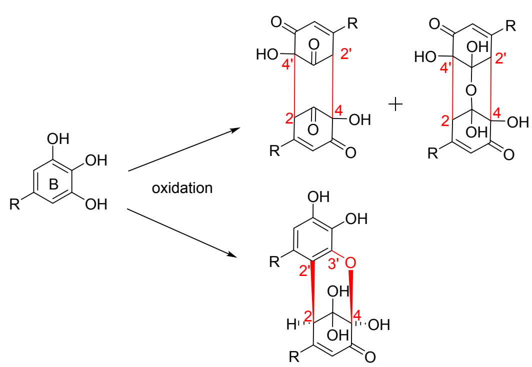

KEYWORDS: Catechins, Flavanols, Natural product, Mechanistic study, Polyphenols, DFT

INTRODUCTION

Catechins are polyphenols that are abundant in tea leaves and are known to have various biological effects, including antioxidant and antitumor activities.[1,2] In the manufacture of oolong and black teas, the catechins present in the tea leaves are oxidized by polyphenol oxidase, resulting in the formation of dimers, such as theaflavin, theasinensin, and oolongtheanin.[3,4,5] These compounds are characteristic catechin dimers; they are formed by condensation reactions between the B-rings (see Scheme 1) and have been predicted to exert various bioactive effects.[6] Therefore, we have previously investigated the formation mechanism of theaflavins and oolongtheanins from catechins.[7,8] Because these compounds are products of the condensation reaction between B-rings, the oxidation reaction mechanism was investigated using catechol and pyrogallol derivatives as model catechins. Previously, it has been shown that benzotropolone derivatives, which represent part of the structure of theaflavins, are obtained by oxidative condensation reaction between 5-methylpyrogallol (**1**) (see Scheme 1 for labeling scheme), corresponding to pyrogallol-type catechin (EGC or EGCg), and 4-methylcatechol (**2**), corresponding to catechol-type catechin (EC or ECg).[8] On the other hand, compounds **4** and **5** are obtained by the oxidative self-condensation reaction of 5-methylpyrogallol (**1**).

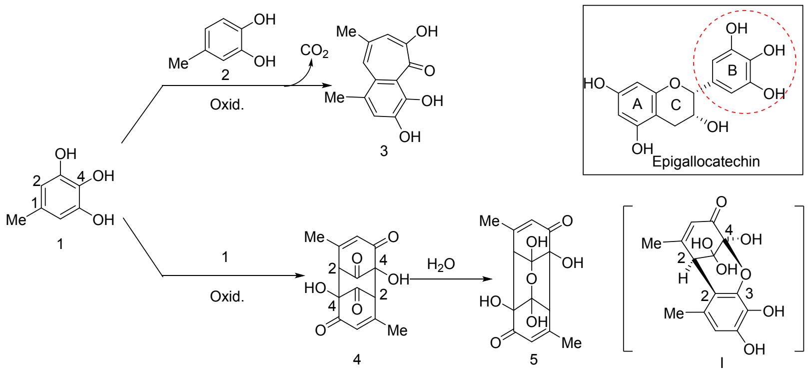

Scheme 1. Oxidation products of **1** and **2**.

Theasinensin and oolongtheanine are formed by the 2C-2C bond formation between the B-rings of two molecules of EGC in the presence of copper chloride.[9] These dimers are known to be condensates of pyrogallol-type catechin and account for the major product of the condensation reactions. In contrast, **4** and **5** (Scheme 1) contain two 2C-4C bonds between the two B-rings and account for over 50% of the product yield. Thus, it has been suggested that the difference in reaction between real catechins and **1** may be influenced by the steric hindrance or interactions between molecules. Hence, in this study, we investigated the effect of oxidative condensation on the regioselectivity of the product using various pyrogallol analogs. As shown in Figure 1, simplified substituents on the pyrogallol-type B-ring were used. To determine the effects of the A-ring, **1a**, which does not contain an A-ring, was prepared. To determine the effect of the C-ring oxygen, compound **1b** was used; **1b** contains a carbon chain but no oxygen atom. Additional substituents (**1c** and **1d**) were used to isolate the structural effects further. To understand the mechanism further, we used density functional theory (DFT) calculations. DFT is a commonly used quantum chemistry technique for determining molecular structures and elucidating reactivity.[10,11] In addition, chemical parameters such as the highest orbital molecular orbital (HOMO) and lowest unoccupied molecular orbital (LUMO) energies, HOMO–LUMO gap, chemical hardness, and electrophilicity can be obtained from DFT calculations and can be used to understand the chemical, kinetic, and thermodynamic behavior of molecules and reactions, thus allowing us to clarify the relationship between the calculation reaction parameters, reactivity, and reaction yield.

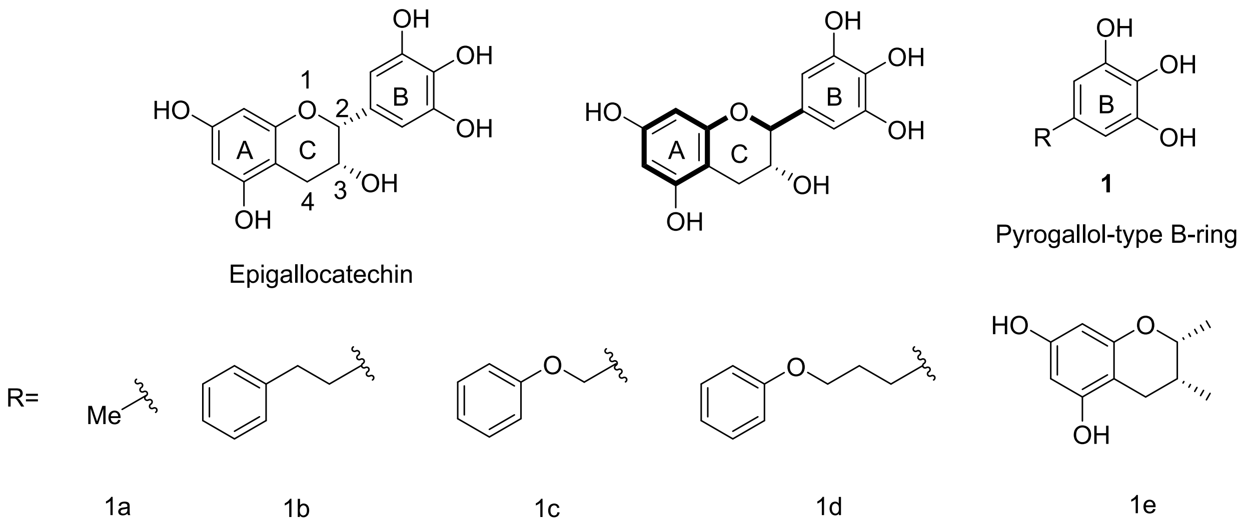

Figure 1. Catechin (top left) showing C-ring numbering and the framework in bold (top middle) chosen for our model compounds. The R-group substituent on the B-ring (top right) was varied from methyl to those containing A-ring substituents with various chain lengths within and without oxygen; the chain acted as a C-ring mimic (bottom).

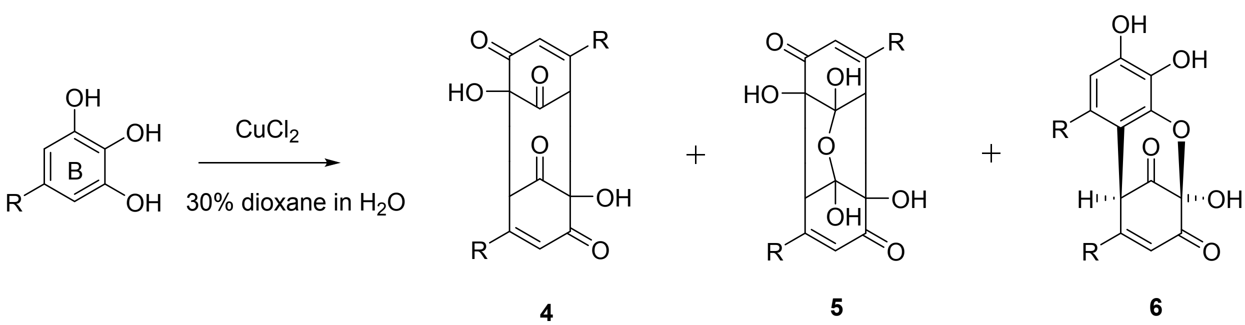

Scheme 2. Oxidation reactions carried out in the presence of copper chloride in aqueous dioxane. The possible products are represented by compounds **4** and **5**, which contain 2C-4C bonds, and compound **6**, which contains 2C-2C bonds.

RESULTS AND DISCUSSION

Compounds **1a**–**1d** were synthesized using modified literature methods. The NMR and mass spectrometry (MS) data of the synthesized compounds already reported were in agreement with the literature values (Schemes S1–S4).[12-23] Compound **1a** has a simple methyl group substituent (see Figure 1 for the labeling figure) and was oxidized with 1 eq of copper chloride in 30% dioxane in water. After removing the copper chloride using an HP20SS column and subjecting the crude products to high-performance liquid chromatography (HPLC) analysis, the three main products were isolated and determined to be **4a**, **5a**, and **6a** by instrumental analysis (see Scheme 2). The product ratio of 2C-4C and 2C-2C-type compounds was 1.1:1, as determined by NMR peak integration (Table 1, Figure S1A). As shown in Scheme 2, compounds **4** and **5** contain 2C-4C bonds and **6** contains a 2C-2C bond, so there was no regioselective effect in this reaction. Thus, we concluded that the A- and C-rings are involved in determining the regioselectivity, especially considering that, when **1e** was used **4e** and **5e** were generated in over 50% yield. Therefore, to investigate the influence of the A-ring on the regioselectivity in the condensation reaction, the oxidation reaction of **1b** was again carried out with 1 eq of copper chloride and 30% dioxane in water. After removing the copper chloride and subjecting the crude mixture to HPLC analysis, **4b**, **5b**, and **6b** were identified as the main products by instrumental analysis. Compound **5b** is a water adduct of **4b**. Further, from the NMR integrals, the product ratio of 2C-4C and 2C-2C-type compounds was 0.7:1 (Table 1, Figure S1B). Because of the presence of the A-ring in the R-group substituent in **1b** but the lack of C-ring oxygen atom, we suggest that the A-ring is important for the selective formation of the 2C-2C bond.

Matsuo et al*.* reported that the stereoselectivity in the oxidative condensation of **1e** is due to the stacking of A-rings because of the hydrophobic effect and π-π interactions. They showed that solvent molecules are located between the A-rings by comparison of the measured and calculated electronic circular dichroism (ECD) spectra of **6e**, which is an oxidative condensate of **1e**, in acetone and acetonitrile.[24] When a large amount of organic solvent is present, the interactions between the A-rings are obstructed, and the regioselective effect is lost. In fact, when **1b** was used for the oxidation reaction in 80% aqueous dioxane solution, the **4b**:**6b** ratio was 1.69:1; that is, the production of **6b** was considerably decreased. Therefore, the A-ring is crucial for the production of compound **6**.

Next, the oxidation reaction of **1c**, which is used a model compound having an oxygen atom corresponding to the 1-position of the C-ring of EGC was performed under the same conditions as that of **1b**. When the reaction mixture of **1c** was subjected to HPLC analysis, two main peaks were observed. Each product was isolated by HPLC, and various NMR and MS analyses were performed. The products were **4c** and **6c**. From the NMR integrals, the product ratio of 2C-4C and 2C-2C-type compounds was found to be 0.45:1 (Table 1, Figure S1C). These results indicate that the oxygen atom at the 1-position of the C-ring, as well as the presence of the A-ring, enhance the formation of the 2C-2C-type compound.

Table 1. Ratios of oxidation product of each compound as determined by NMR.

1	**4** or **5*** (2C-4C)	**6*** (2C-2C)
1a	1.1	1
1b	0.7	1
1c	0.45	1
1d	1.43	1

1e	0	1

*Ratio calculated from ^{1}H-NMR measurements.

The oxidation reactions of **1b** and **1c**, for which 2C-2C-type compounds were predominantly formed, were followed using HPLC, and it was found that 2C-4C-type compounds **4** and **5** were produced in the early stages of the reaction. However, 2C-2C-type products were formed with increasing reaction time. In the presence of a large excess of copper chloride, the reaction was rapid, and **4** and **5** were obtained as the main products (Table 2). In contrast, when using less than one equivalent of copper chloride, the reaction rate was slow, and the amount of 2C-2C-type compound **6** increased (Table 2). These results suggest that the 2C-2C and 2C-4C-type compounds are formed by different routes. When the oxidant is used in high concentrations, as well as in the initial stages of the reaction, condensation between the highly reactive *o*-quinones formed by oxidation occurs because *o*-quinones are produced in large quantities (Scheme 3). On the other hand, the reaction between *o*-quinone and hydroquinone increases as the reaction time increases. Thus, we proposed that the formation of the 2C-4C bond involves a reaction between *o*-quinones, which are oxides of **1**, and the 2C-2C bonds are formed by reactions between *o*-quinone and hydroquinone.

Table 2. Oxidation product ratios depending on $CuCl_2$ equivalents used.

$CuCl_2$ (eq)	**4c***	**6c***
0.3	0.7	1
1	0.85	1
3	1.2	1

*Ratio calculated from ^{1}H-NMR measurements.

The reaction mechanism for the formation of 2C-2C and 2C-4C-type compounds can be regarded as a nucleophilic addition reaction to α,β-unsaturated ketones. That is, the formation of 2C-4C bonds involves the direct addition (1,2-addition) to a ketone, whereas the formation of the 2C-2C bonds involves a conjugate addition (1,4-addition) reaction. In addition, in reactions of α,β- unsaturated ketones, direct and conjugate addition reactions result in the kinetic and thermodynamic products, respectively. This is because the addition reaction to the ketone is usually reversible, so the final product is the thermodynamic conjugate addition product. However, **4** and **5** were obtained as products because these compounds are relatively stable when two direct addition reactions occur simultaneously (Scheme 3).

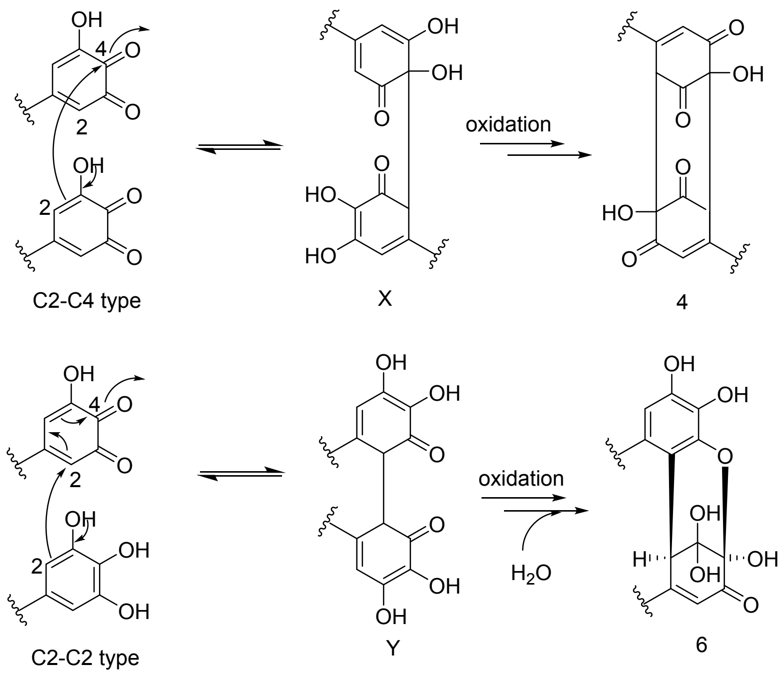

Scheme 3. Direct addition (1,2-addition) and conjugate addition (1,4-addition) reactions.

Next, the oxidation of **1d** was carried out under the same conditions as those for **1b**. When the reaction mixture was subjected to HPLC analysis, multiple peaks were observed in addition to the two main peaks. Each peak was isolated by HPLC and various NMR and MS analyses were carried out. The two main products were **4d** (2C-4C) and **6d** (2C-2C). Based on the ^{1}H-NMR integrals, the product ratio of 2C-4C and 2C-2C-type products is 1.43:1 (Table 1, Figure S1D). Despite having an oxygen atom like **1c**, **1d** showed reactivity similar to that of **1b**. Furthermore, when the rates of oxidation of **1a** to

1e were compared, the order was found to be **1a** > **1d** = **1b** > **1e** > **1c** (Figure 2). Compound **1d** contains oxygen in the R-group substituent, but no enhancement effect of the oxygen atom on the regioselectivity of the reaction was observed. Further, its reactivity is similar to that of compound **1b**, whose R-group substituent does not contain oxygen.

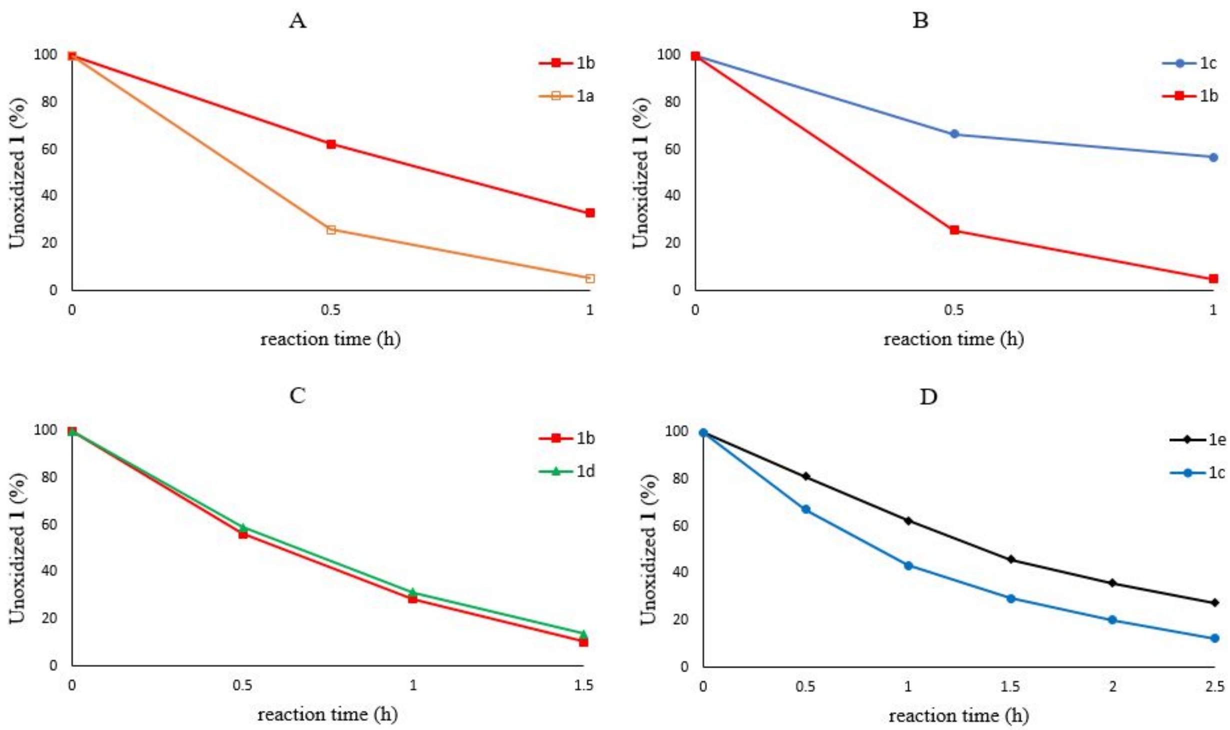

Figure 2. Rates of oxidation of A (**1a** and **1b**), B (**1b** and **1d**), C (**1b** and **1c**), and D (**1c** and **1e**).

The difference between compounds **1c** and **1d** is the distance from the oxygen atom to the B-ring. The oxygen atom of **1c** is closer to the B-ring than that in **1d**. Thus, this oxygen atom may affect the rate of the nucleophilic addition reaction at the B-ring.

Next, we used DFT to study the reactivity and redox properties of the compounds formed by oxidation and condensation. Concerning redox chemistry, a lower HOMO energy indicates easier oxidation.[25] The experimentally obtained oxidation rates for **1a**–**e** decrease in order **1a** > **1b** = **1d** > **1c** > **1e** (Figure 2), and the calculated HOMO energies of all hydroquinone compounds are **1a** > **1b** = **1d** > **1e** > **1c**. Thus, the presence of the oxygen atom at the 1-position of the C-ring increased the HOMO energy and reduced the rate of oxidation (Table 3). The oxidation reaction can also be evaluated by the ionization potential (I) and electrophilicity (ω). When the ionization energy is low, a compound is easily oxidized.[26] Further, when the electrophilicity of a compound is high, its oxidation is harder.[27] Thus, I and ω of the hydroquinone compounds were calculated and were found to increase in order **1a** < **1b** = **1d** < **1e** < **1c** (Table 3). These results indicate that **1c** is less susceptible to oxidation than the other compounds. Further, the calculations show that **1a**, **1b**, and **1d** are more likely to be oxidized and form *o*-quinones than **1c** and **1e**. As shown in Table 3, the former tended to form 2C-4C-type products, whereas the latter tended to form 2C-2C-type products. On the basis of these results, if **1** is easily oxidized, the probability of *o*-quinone formation increases, so that the reaction proceeds between *o*-quinones to form 2C-4C-type products. On the other hand, if **1** is relatively difficult to oxidize, the formation of *o*-quinone is less likely; thus, the reaction between the *o*-quinone and hydroquinone proceeds to form 2C-2C-type products.

Table 3. DFT calculated parameters for **1a** to **1e**.

	E_{HOMO} (eV)	E_{LUMO} (eV)	ΔE (eV)	I (eV)	A (eV)	η (eV)	χ (eV)	ω (eV)	ε
1a	-5.58	0.389	5.97	5.58	-0.389	2.98	2.6	10.0	-0.435
1b	-5.61	-0.0955	5.52	5.61	0.0955	2.76	2.85	11.2	-0.517
1c	-5.82	-0.0999	5.72	5.82	0.0999	2.86	2.96	12.5	-0.517

1d	-5.61	-0.0914	5.52	5.61	0.0914	2.76	2.85	11.2	-0.517
1e	-5.75	0.0473	5.79	5.75	-0.0473	2.90	2.85	11.8	-0.492

Next, the reaction enthalpies of the **1a**–**e** ($\Delta_r H_{(X\text{-}1)}$ or $\Delta_r H_{(Y\text{-}1)}$) and the differences between the enthalpies of these products ($\Delta_r H_{(X\text{-}1)}$-$\Delta_r H_{(Y\text{-}1)}$) were calculated. Using these values, we compared the thermodynamic stability of **4** and **6** and evaluated their reactivity. Because the formation of **6** increased when the A-ring substituent was used, as well as with the R substituents containing oxygen (see Table 1), we expected that **6** would be more thermodynamically stable. Therefore, the changes in the thermodynamic stability of **6** with changes in the R-group substituent were investigated. Although it is not possible to compare the enthalpies of the products directly, we compared the enthalpies of products of X and Y, which are reaction intermediates of **4** and **6** having the same molecular weight, to estimate their thermodynamic stabilities.

Table 4. Enthalpy changes of compounds with substituents **a**–**e**.

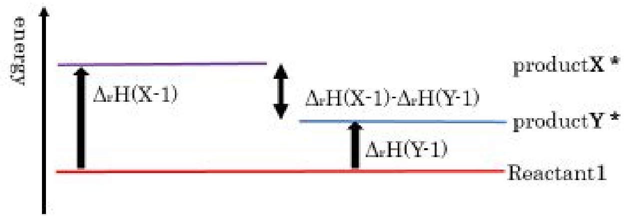

R	$\Delta_r H_{(X\text{-}1)}$/(kcal mol^{-1})	$\Delta_r H_{(Y\text{-}1)}$/(kcal mol^{-1})	$\Delta_r H_{(X\text{-}1)} - \Delta_r H_{(Y\text{-}1)}$/(kcal mol^{-1})
A	770.06	763.14	6.92
B	775.14	765.81	9.33
C	774.01	764.03	9.98
D	774.18	765.77	8.41
E	765.85	767.49	-1.65

*Structures of X and Y are given in Scheme 3.

In general, a lower value of $\Delta_r H_{(X\text{-}1)}$ or $\Delta_r H_{(Y\text{-}1)}$ indicates stability, and, thus, the oxidation product is more easily generated. For compounds **1a**–**d**, $\Delta_r H_{(X\text{-}1)}$ was greater than $\Delta_r H_{(Y\text{-}1)}$, suggesting that intermediate **Y** was more thermodynamically stable (Table 4).

Therefore, we speculate that the larger reaction enthalpy difference ($\Delta_r H_{(X\text{-}1)} - \Delta_r H_{(Y\text{-}1)}$) between the products indicates a higher product ratio of **6**. The values of $\Delta_r H_{(X\text{-}1)} - \Delta_r H_{(Y\text{-}1)}$ are very different for **1a** and **1e**, especially **1b**, which contains an A-ring, and **1c**, which has an oxygen atom at the 1-position of the model C-ring, for which the values are very high (Table 4). These results appear to confirm the results of previous studies concerning the π-π stacking interactions of the A-ring, as well as the importance of the C-ring oxygen atom, both of which may enhance the stability of **6**. Further, we suggest that the thermodynamically stable 1,4-addition reaction proceeds preferentially over the kinetically dominant 1,2-addition. Like **1b** and **1c**, **1d** also contains an A-ring and oxygen atom, but the larger distance between the A- and B-rings results in greater flexibility. Possibly, the increase in flexibility decreases the regioselectivity of the reaction between the B-ring, and, thus, the products of 1,4-addition decrease. Concerning **1e**, the thermodynamic stability of the **X** intermediate is higher than that of the **Y** intermediate. This is probably because the structure of **1e** is significantly different from those of **1a**–**d**.

CONCLUSIONS

We have found that the A-ring and the oxygen atom at the 1-position of the C-ring affect the regioselectivity in the oxidative condensation of the catechin B-ring. Experimental results and DFT calculations suggest that the HOMO energy of ring B which is affected by the oxygen atom at 1-position of the C-ring, and the thermodynamic stability of the product are all important. These results suggests that the whole catechin molecule is involved in the reactivity of the B-ring and that the reaction is regioselective. Although there have been many reports on the functionality of polyphenols including catechins, there is significant scope for further investigation, and many compounds, for example, high-molecular-weight polyphenols in fermented tea, remain uninvestigated. We believe that the findings obtained here will contribute to the elucidation of the reaction mechanism of the oxidation of tea catechins and the chemical structure of polymeric polyphenols.

EXPERIMENTAL SECTION

Chemicals. EGCg was gifted by Nagara Science Co. (Gifu, Japan). EGC was prepared from EGCg by enzyme reaction using a tannase.[9] Dioxane and tetrahydrofuran (THF) were purchased from FUJIFILM Wako pure Chemical Corporation (Osaka, Japan). Deuterated dimethyl sulfoxide (DMSO-d_6) and D_2O were purchased from KANTO

CHEMICAL Corporation (Tokyo, Japan). Acetone-*d*$_6$ was purchased from ACROS ORGANICS Corporation (Tokyo, Japan).

General procedure for oxidative condensation

Compounds **1a** to **1d** were oxidatively condensed using the following method. First, 400 μL of 30% dioxane aqueous solution was added to 2 mg (0.014 mmol) of **1a** and stirred until the solid dissolved. Then, 2.4 mg (0.014 mmol) of $CuCl_2{\cdot}2H_2O$ dissolved in 400 μL of 30% dioxane aqueous solution was added, and the mixture was stirred at room temperature for 2 h. After the reaction had completed, the $CuCl_2{\cdot}2H_2O$ was removed using a Diaion HP20SS resin column (Mitsubishi Chemical Co., Japan), which had been washed with water, and all compounds were eluted with MeCN and concentrated. The same procedure was performed for **1b**–**d**. **1e** was prepared by the same procedure as above except that 30% THF aqueous solution was used.

Measurement of the oxidation rates of 1a–e

For these experiments, **1a** (1.5 mg, 0.0065 mmol), **1b** (0.91 mg, 0.0065 mmol), and $CuCl_2{\cdot}2H_2O$ (1.1 mg, 0.0065 mmol) were added to 400 μL of 30% dioxane aqueous solution, and the mixture was stirred at room temperature until the raw materials disappeared. The reaction was monitored by HPLC every 30 min, and the remaining proportion of the model compound was evaluated by considering the peak area before reaction as 100%. The same procedure was performed for **1b** and **1d**, **1d** and **1c**, and **1c** and **1e**. HPLC analysis of each sample was carried out with a JASCO PU-2080 intelligent pump equipped with a JASCO UV-2075 intelligent UV/VIS detector and Sugai U-620 column heater (Tokyo, Japan). The HPLC conditions were as follows. The sample (5 μL) was injected onto a COSMOSIL C18 column (Cosmosil 5C18-MS-Ⅱ 4.6 mm I.D. × 150 mm, Nacalai Tesque Co., Ltd., Kyoto, Japan). The oven temperature was maintained at 35 °C. The eluents for the compounds were as follows: for **1a** and **1b**, 25% acetonitrile, 0.5% formic acid, and 74.5% water; for **1b** and **1d**, 42% acetonitrile, 0.5% formic acid, and 57.5% water; for **1c** and **1d**, 42% acetonitrile, 0.5% formic acid, 57.5% water; and, for **1c** and **1e**, 20% acetonitrile 0.5% formic acid 79.5% water. The flow rate was maintained at 1.0 mL/min, and the eluted compounds were monitored at 254 nm.

Determination of ratio of oxidation product formation by NMR

The oxidation product of **1a** was dissolved in 0.2 mL of DMSO-d_6 + 1 drop D_2O, and ^{1}H-NMR measurements were performed. **1b–e** were dissolved in 0.2 mL of acetone-d_6 + 1 drop D_2O and subjected to ^{1}H-NMR measurements. ^{1}H-NMR spectra were recorded on a JEOL ECA 500 (JEOL, Japan) at 500 MHz and a JEOL ECA 600 (JEOL, Japan) at 600

MHz. The product ratio was calculated by averaging the integrated values of the peaks at 5.8–6.3 and 3.7–4.3 ppm (hydrogen atoms in the condensed B-ring) that did not overlap with other peaks. When compound **1** was used, the integrals with respect to **4** and **5** represent 2H, so the integrated value was divided by 2 to obtain the product ratio. The NMR data of each oxidation product can be found in the Supplementary Information.

MS spectra instrument

Mass of all compounds were measured using JMS-700 (JEOL, Japan), AccuTOF (JEOL, Japan), UPLC-QTOF-MS (Waters Xevo G2 QTOF, Waters, USA).

Compound 1c synthetic methods

A solution of 5-phenoxy-1,2,3-tris[[(1,1-dimethylethyl)dimethylsilyl]oxy]-benzene crude in anhydrous THF (12 ml) was added 1M TBAF in THF (1.02 ml) and stirred at room temperature for 1h in argon conditions. After 1 hour, saturated saline was added, and the mixture was extracted with EtOAc. The combined organic layers were washed with brine, dried over Na_2SO_4 and concentrated in vacuo. After concentration, Column chromatography (EtOAc/n-hexane = 1:1) gave compound **1c** as a white solid (80 mg, 38.8%, 2step).

^{1}H-NMR (600MHz, acetone-d_6) δ (ppm): 7.26 (2H, t, 7.56Hz, C-5', 7'), 6.96 (2H, d, 7.56Hz, C-4', 8'), 6.90 (1H, t, 7.56Hz, C-6'), 6.50 (2H, s, C-2), 4.89 (2H, S, C-1'), ^{13}C {^{1}H} NMR (150MHz, acetone-d_6) δ (ppm): 159.8 (C-3'), 146.5 (C-4), 133.2 (C-3, 5), 130.1 (C-5', 7'), 129.3 (C-1), 121.3 (C-6'), 115.6 (C-4' 8'), 107.6 (C-2), 70.3 (C-1), LCMS (ESI) *m/z* : calcd for $C_{13}H_{12}O_4$ 231.0657 ; Found 231.0629 $(M-H)^-$

Compound 1d synthetic methods

A solution of 5-(3-phenoxypropyl)-1,2,3-tris(phenylmethoxy)-benzene (360 mg, 0.68 mmol) in MeOH/CH_2Cl_2 = 1:1 (1 ml) was added 10% Pd/C (36 mg) and stirred at room temperature for 1h30min under conditions filled with hydrogen. After the reaction was completed, the mixed solution was filtered through Celite to remove 10% Pd/C and concentrated in vacuo. After concentration, Column chromatography (EtOAc/n-hexane = 2:3) gave compound **1d** as a white solid (120 mg, 68.0%).

^{1}H-NMR (500MHz, acetone-d_6) δ (ppm): 7.26 (2H, t, 7Hz, C-7', 9'), 6.92-6.89 (3H, m, C-6', 8', 10'), 6.28 (2H, s, C-2, 6), 3.96 (2H, t, 6.5Hz, C-3'), 2.59 (2H, t, 7.5Hz, C-1'), 2.02-1.97 (2H, m, C-2'), ^{13}C {^{1}H} NMR (125MHz, acetone-d_6) δ (ppm):160.0 (C-5'), 146.6 (C-3), 133.6 (C-1), 131.6 (C-4), 130.2 (C-7', 9'), 121.2 (C-6', 10'), 115.3 (C-8'), 108.1 (C-2, 6), 67.5 (C-3'), 32.3 (C-1'), 31.8 (C-2'), LCMS (ESI) *m/z* : calcd for $C_15H_{16}O_4$ 259.0970 ; Found 259.0925 $(M-H)^-$

NMR chemical shift values and MS values of oxidation products of each model compound

4a: white solid ^{1}H-NMR (600MHz, d_6-DMSO) δ (ppm): 7.02 (2H, s, OH) 6.23 (2H, s, C-6), 3.48 (2H, s, C-2), 2.20 (6H, s, C-7), ^{13}C {^{1}H} NMR (150MHz, d_6-DMSO) δ (ppm): 198.6 (C-3), 193.8 (C-5), 161.8 (C-1), 126.0 (C-6), 88.3 (C-4), 62.6 (C-2), 25.5 (C-7), LCMS (ESI) *m/z* : calcd for $C_{14}H_{12}O_6$ 275.0556 ; Found 275.0518 $(M-H)^-$

5a: yellow solid ^{1}H-NMR (600MHz, d_4-MeOD) δ (ppm): 6.01 (2H, s, C-6), 3.02 (2H, s, C-2), 1.89 (6H, s, C-7), ^{13}C {^{1}H} NMR (150MHz, d_4-MeOD) δ (ppm): 197.5 (C-5), 160.2 (C-1), 128.3 (C-6), 105.3 (C-3), 85.9 (C-4), 65.6 (C-2), 24.7 (C-7), LCMS (ESI) *m/z* : calcd for $C_{14}H_{14}O_7$ 293.0661 Found 293.0689 $(M-H)^-$

6a: white solid ^{1}H-NMR (600MHz, d_4-MeOD) δ (ppm): 6.30 (1H, s, C-6'), 5.87 (1H, s, C-6), 3.75 (1H, s, C-2), 2.31 (3H, s, C-7'), 2.08 (3H, s, C-7), ^{13}C {^{1}H} NMR (150MHz, d_4-MeOD) δ (ppm): 193.0 (C-5), 167.2 (C-1), 146.1 (C-5'), 143.2 (C-3'), 132.0 (C-4'), 126.2 (C-1'), 122.4 (C-6), 114.4 (C-6'), 111.1 (C-2'), 96.4 (C-4), 92.0 (C-3), 49.8 (C-2), 24.2 (C-7), 19.0 (C-7'), LCMS (ESI) *m/z* : calcd for $C_{14}H_{14}O_7$ 293.0661 Found 293.0689 $(M-H)^-$

4b: white solid ^{1}H-NMR (600MHz, d_6-acetone) δ (ppm): 7.28-7.18 (10H, m, C-3'~8'), 6.19 (2H, s, C-5), 5.78 (2H, s, OH), 3.64 (2H, s, C-2), 3.06-2.83 (8H, m, C1', 2'), ^{13}C {^{1}H} NMR (150MHz, acetone-d_6) δ (ppm): 197.8 (C-3), 193.8 (C-5), 165.1 (C-1), 141.2 (C-3'), 129.3 (C-5'), 129.2 (C-4'), 127.0 (C-6'), 126.1 (C-6), 89.7 (C-4), 63.2 (C-2), 40.6 (C-1'), 33.3 (C-2'), LCMS (ESI) *m/z* : calcd for $C_{28}H_{24}O_6$ 457.1651 Found 457.1628 $(M+H)^+$

5b: yellow solid ^{1}H-NMR (600MHz, d_6-acetone) δ (ppm): 7.31-7.12 (10H, m, C-3'~8'), 5.97 (2H, s, C-6), 3.24 (2H, s, C-2), 3.02-2.84 (2H, m, C1', 2'), 2.67-2.61 (2H, m, C1', 2'), 2.51-2.35 (4H, m, C1', 2'), ^{13}C {^{1}H} NMR (150MHz, acetone- d_6) δ (ppm): 195.7 (C-5), 160.9 (C-1), 140.2 (C-3'), 128.0 (C-5'), 127.6 (C-4'), 125.8 (C-6'), 125.7 (C-6), 103.6 (C-3), 84.5 (C-4), 62.7 (C-2), 37.9 (C-1'), 31.5 (C-2'), LCMS (ESI) *m/z* : calcd for C28H26O7 513.1316 Found 513.1326 $(M+K)^+$

6b: white solid ^{1}H-NMR (600MHz, d_6-acetone) δ (ppm): 7.28-7.14 (10H, m, C-3''~8'', C3'''~8'''), 6.48 (1H, s, C-6'), 5.92 (1H, s, C-6), 4.09 (1H, s, C-2), 3.09-2.95 (2H, m, C1', 2'), 2.85-2.60 (6H, m, C1', 2'), ^{13}C {^{1}H} NMR (150MHz, acetone- d_6) δ (ppm): 192.2 (C-5), 168.2 (C-1), 145.7 (C-4'), 142.7 (C-3'',C-3'''), 141.4 (C-1'), 131.7 (C-5'), 129.6 (C-3'), 129.0, 128.9, 128.8, 126.8, 126.5, 126.1(C-4''~8'', C-4''' ~8'''), 120.9 (C-6), 113.6 (C-2'), 109.6 (C-6’), 96.0 (C-4), 91.7 (C-3), 47.6 (C-2), 38.6 (C-1’’), 38.3 (C-2’’’), 35.3 (C-1’’’), 33.3 (C-2’’), LCMS (ESI) *m/z* : calcd for $C_{28}H_{26}O_7$ 513.1316 Found 513.1326 $(M+K)^+$

4c: white solid ^{1}H-NMR (600MHz, d_6-acetone) δ (ppm): 7.32 (4H, dd, 7.56Hz, 8.22Hz, C-5’), 7.05 (4H, d, 8.22Hz, C-4’), 6.99 (2H, t, 7.56Hz, C-6’), 6.42 (2H, s, C-6) 5.28-5.25 (1H, d, 2.04Hz, C-1’), 5.05-5.02 (1H, d, 2.04Hz, C-1’), 3.76(2H, s, C-2), ^{13}C {^{1}H} NMR (150MHz, acetone- d_6) δ (ppm): 196.9 (C-3), 193.1 (C-5), 160.0 (C-1), 158.5 (C-3’), 130.5 (C-5’), 124.4 (C-6), 122.4 (C-4’), 115.6 (C-6’), 89.8 (C-4), 69.9 (C-1’), 60.1 (C-2), LCMS (ESI) *m/z* : calcd for $C_{26}H_{20}O_8$ 459.1080 Found 459.1103 $(M-H)^-$

6c: white solid ^{1}H-NMR (600MHz, d_6-acetone) δ (ppm): 7.28 (2H, dd, 7.56Hz, 8.22Hz, C-5’’), 7.18 (2H, dd, 7.56Hz, 8.22Hz, C-5’’’), 6.99 (2H, d, 7.56Hz, C-4’’), 6.97 (1H, t, 7.56Hz, C-4’’’), 6.93 (1H, t, 7.56Hz, C-6’’), 6.80 (2H, d, 8.28Hz, C-6’’’), 6.70 (1H, s, C-6’), 6.23 (1H, s, C-6), 5.13 (1H, d, 10.32Hz, C-1’), 5.04 (1H, d, 10.98Hz, C-1’’), 4.99 (1H, d, 1.38Hz, C-1’’’), 4.84 (1H, dd, 1.38Hz, 16.44Hz, C-1’’’), 4.19 (1H,s, C-2), ^{13}C {^{1}H} NMR (150MHz, acetone- d_6) δ (ppm): 191.4 (C-5), 163.2 (C-1), 159.6 (C-3’’), 158.6 (C-3’’’), 146.3 (C-5’), 143.0 (C-1’), 133.8 (C-4’), 130.3 (C-5’’,7’’, 5’’’, 7’’’), 125.1 (C-3’), 122.0 (C-6’’’), 120.1 (C-6’’), 120.0 (C-6), 115.6 (C-4’’, 8’’), 115.4 (C-4’’’, 8’’’), 114.6 (C-2’), 111.1 (C-

6'), 96.6 (C-4), 91.9 (C-3), 68.3 (C-1''), 67.6 (C-1'''), 44.9 (C-2), LCMS (ESI) *m/z* : calcd for $C_{26}H_{22}O_9$ 477.1161 Found 477.1161 $(M-H)^-$

4d: white solid ^{1}H-NMR (600MHz, d_6-acetone) δ (ppm): 7.26 (4H, t, 7.8Hz, C-7', 9), 6.91 (6H, m, C-6', 8', 10'), 6.27 (2H, s, C-6), 4.03 (2H, t, 6Hz, C-3'), 3.66 (1H, s, C-2), 2.95-2.80 (2H, m, C-1'), 2.18-2.00 (2H, m, C-2'), ^{13}C {^{1}H} NMR (150MHz, acetone- d_6) δ (ppm): 198.1 (C-5), 193.9 (C-3), 165.5 (C-1), 159.8 (C-5'), 130.2 (C-7'), 125.9 (C-6), 121.4(C-6'), 115.3 (C-8'), 89.8 (C-4), 67.5 (C-3'), 63.2 (C-2), 35.9 (C-1'), 27.1 (C-2'), LCMS (ESI) *m/z* : calcd for $C_{30}H_{28}O_8$ 515.1706 Found 515.1726 $(M-H)^-$

6d: white solid ^{1}H-NMR (600MHz, d_6-acetone) δ (ppm): 7.24 (4H, t, 9Hz, C-7', 9'), 6.95 (2H, d, 9.6Hz, C-8'), 6.90 (4H, d, 7.2Hz, 6', 8'), 6.43 (1H, s, C-6'), 5.94 (1H, s, 6), 4.15-3.95 (5H, m, C-2, C-3''), 3.03-2.97 (1H, m, C-3'', 3'''), 2.72-2.66 (1H, m, C-3'', 3'''), 2.62-2.57 (1H, m, C-3'', 3'''), 2.57-2.50 (1H, m, C-3'', 3'''), 2.19-2.02 (4H,m, C-2'',2'''), ^{13}C {^{1}H} NMR (150MHz, acetone- d_6) δ (ppm): 191.8 (C-5), 168.8 (C-6), 160.1 (C-5''), 159.9 (C-5'''), 146.1 (C-6'), 143.0 (C-4'), 131.8 (C-5'), 130.3 (C-7'', 9'', 7''', 9'''), 121.3 (C-6'', 10'' ,6''', 10'''), 115.4 (C-8'',8'''), 114.1 (C-2'), 109.7 (C-6'), 96.1 (C-4), 92.1 (C-3), 67.7 (C-3'''), 67.3 (C-3''), 47.7 (C-2), 33.2 (C-2'''), 32.2 (C-1'''), 29.3 (C-1'') 27.3 (C-2''), LCMS (ESI) *m/z* : calcd for $C_{30}H_{30}O_9$ 533.1812 Found 533.1824 $(M-H)^-$

Computational details

CONFLEX 8 Rev.C (CONFLEX, Japan) was used to search the conformations of **1a**–**e** and the intermediates and products formed by their oxidative condensation.[28,29] After conformational searching using the MMFF94s force field, many initial conformers were identified. All stable conformers with a population of over 1% were chosen. Selected conformers were optimized in the gas phase using the semi-empirical PM6 method in Gaussian16W (Gaussian, Japan).[30-34] Next, the minimum energy conformer calculated using the PM6 method was optimized in water using the polarizable continuum model at the B3LYP/6-31G** level of theory in Gaussian16W. To determine that the optimized reactants, intermediates, and products were true minima, frequency calculations at the same level of theory as the optimization calculations were carried out. Finally, using the obtained data, the thermodynamic parameters were obtained.

ASSOCIATED CONTENT

Supporting Information

Schemes of synthetic routes for the model compounds. Synthetic methods for preparation of model compounds. NMR and MS data for products of oxidation. Coordinates of DFT optimized structures and frequency calculation results.

The Supporting Information is available free of charge at http://pubs.acs.org.

AUTHOR INFORMATION

Corresponding Author

Emiko Yanase – Faculty of Applied Biological Sciences, Gifu University, 1-1 Yanagido, Gifu 501-1193, Japan

*Tel. and Fax: +08-58-293-2914. E-mail: e-yanase@gifu-u.ac. jp.

Authors

Yuto Ochiai – Graduate School of Natural Science and Technology, Gifu University, 1-1 Yanagido, Gifu 501-1193, Japan

Sayumi Hirose – Graduate School of Natural Science and Technology, Gifu University, 1-1 Yanagido, Gifu 501-1193, Japan

Emiko Yanase – Faculty of Applied Biological Sciences, Gifu University, 1-1 Yanagido, Gifu 501-1193, Japan

REFERENCES

(1) Nanjo, F.; Honda, M.; Okushio, K.; Matsumoto, N.; Ishigaki, F.; Ishigami, T.; Hara, Y. Effects of Dietary Tea Catechins on α-Tocopherol Levels, Lipid Peroxidation, and Erythrocyte Deformability in Rats Fed on High Palm Oil and Perilla Oil Diets. *Biol. Pharm. Bull.* **1993**, *16* (11), 1156–1159. https://doi.org/10.1248/bpb.16.1156.

(2) Sharangi, A. B. Medicinal and Therapeutic Potentialities of Tea (*Camellia sinensis* L.) - A Review. *Food Res. Int.* **2009**, *42* (5–6), 529–535. https://doi.org/10.1016/j.foodres.2009.01.007.

(3) Takino, Y.; Imagawa, H. Studies on the Mechanism of the Oxidation of Tea Leaf Catechins. *Agric. Biol. Chem.* **1964**, *28* (2), 125–130. https://doi.org/10.1271/bbb1961.28.125.

(4) Nonaka, G. I.; Kawahara, O.; NIshioka, I. Tannins and Related Compounds. XV. A New Class of Dimeric Flavan-3-Ol Gallates, Theasinensins A and B, and

Proanthocyanidin Gallates from Green Tea Leaf. (1). *Chem. Pharm. Bull.* **1983**, *31* (11), 3906–3914. https://doi.org/10.1248/cpb.31.3906.

(5) Hashimoto, F.; Nonaka, G.-I.; Nishioka, I. Tannins and Related Compounds. LXIX. Isolation and Structure Elucidation of B,B'-Linked Bisflavanoids, Theasinensins D-G and Oolongtheanin from Oolong Tea. (2). *Chem. Pharm. Bull.* **1988**, *36* (5), 1676–1684. https://doi.org/10.1248/cpb.36.1676.

(6) Rothenberg, D. O. N.; Zhou, C.; Zhang, L. A Review on the Weight-Loss Effects of Oxidized Tea Polyphenols. *Molecules* **2018**, *23* (5), 1176. https://doi.org/10.3390/molecules23051176.

(7) Hirose, S.; Tomatsu, K.; Yanase, E. Isolation of Key Intermediates during Formation of Oolongtheanins. *Tetrahedron Lett.* **2013**, *54* (51), 7040–7043. https://doi.org/10.1016/j.tetlet.2013.10.069.

(8) Yanase, E.; Sawaki, K.; Nakatsuka, S. I. The Isolation of a Bicyclo[3.2.1] Intermediate during Formation of Benzotropolones, a Common Nucleus Found in Black Tea Pigments: Theaflavins. *Synlett* **2005**, *(17)*, 2661–2663. https://doi.org/10.1055/s-2005-917094.

(9) Hirose, S.; Kamatari, Y. O.; Yanase, E. Mechanism of Oolongtheanin Formation via Three Intermediates. *Tetrahedron Lett.* **2020**, *61* (11), 151601. https://doi.org/10.1016/j.tetlet.2020.151601.

(10) Doi, K.; Sakamoto, T.; Maida, N.; Tachibana, A. Outline of Calculation for Chemical Reactions Using Density-Functional-Theory Method. *Shinku/Journal Vac. Soc. Japan* **2006**, *49* (9), 514–519. https://doi.org/10.3131/jvsj.49.514.

(11) Kohn, W.; Becke, A. D.; Parr, R. G. Density Functional Theory of Electronic Structure. *J. Phys. Chem.* **1996**, *100* (31), 12974–12980. https://doi.org/10.1021/jp960669l.

(12) Bouges, H.; Calabro, K.; Thomas, O. P.; Antoniotti, S. Unusual Polycyclic Fused Product by Oxidative Enzymatic Dimerisation of 5-Methylpyrogallol Catalysed by Horseradish Peroxidase/H_2O_2. *Molecules* **2018**, *23* (10), 2619. https://doi.org/10.3390/molecules23102619.

(13) Wu, Y.-C.; Leowanawat, P.; Sun, H.-J.; Partridge, B. E.; Peterca, M.; Graf, R.; Spiess, H. W.; Zeng, X.; Ungar, G.; Hsu, C.-S.; et al. Complex Columnar Hexagonal Polymorphism in Supramolecular Assemblies of a Semifluorinated Electron-Accepting

Naphthalene Bisimide. *J. Am. Chem. Soc.* **2015**, *137* (2), 807–819. http://dx.doi.org/10.1021/ja510643b.

(14) Ding, T. J.; Wang, X. L.; Cao, X. P. A Fast Assembly of (-)-Epigallocatechin-3-Gallate [(-)-EGCG] via Intra- and Inter-Molecular Mitsunobu Reaction. *Chinese J. Chem.* **2006**, *24* (11), 1618–1624. https://doi.org/10.1002/cjoc.200690303.

(15) Chalal, M.; Vervandier-Fasseur, D.; Meunier, P.; Cattey, H.; Hierso, J. C. Syntheses of Polyfunctionalized Resveratrol Derivatives Using Wittig and Heck Protocols. *Tetrahedron* **2012**, *68* (20), 3899–3907. https://doi.org/10.1016/j.tet.2012.03.025.

(16) Hearn, M. T. W.; Langford, S.; Tuck, K. L.; Harris, S.; Boysen, R. I.; Perchyonok, V. T.; Danylec, B.; Schwarz, L.; Chowdhury, J. Molecularly Imprinted Polymers. WO2010085851A1, 2010.

(17) Sakurai, T.; Tsutsui, Y.; Kato, K.; Takata, M.; Seki, S. Preferential Formation of Columnar Mesophases via Peripheral Modification of Discotic π-Systems with Immiscible Side Chain Pairs. *J. Mater. Chem. C* **2016**, *4* (7), 1490–1496. https://doi.org/10.1039/c6tc00021e.

(18) Song, Y.-O.; Suh, H.; Choi, J. Composition for Treating Arteriosclerosis Comprising 3-(4'-Hydroxyl-3',5'-Dimethoxyphenyl)Propionic Acid or Its Derivatives. WO2002074300A1, 2002.

(19) Reano, A. F.; Chérubin, J.; Peru, A. M. M.; Wang, Q.; Clément, T.; Domenek, S.; Allais, F. Structure-Activity Relationships and Structural Design Optimization of a Series of *p*-Hydroxycinnamic Acids-Based Bis- and Trisphenols as Novel Sustainable Antiradical/Antioxidant Additives. *ACS Sustain. Chem. Eng.* **2015**, *3* (12), 3486–3496. https://doi.org/10.1021/acssuschemeng.5b01281.

(20) Feghali, E.; van de Pas, D. J.; Parrott, A. J.; Torr, K. M. Biobased Epoxy Thermoset Polymers from Depolymerized Native Hardwood Lignin. *ACS Macro Lett.* **2020**, *9*, 1155–1160. https://doi.org/10.1021/acsmacrolett.0c00424.

(21) Cao, X.; Wang, F.; Guo, S. A New Convergent Approach to Dendritic Macromolecules. *Synth. Commun.* **2002**, *32* (20), 3149–3158. https://doi.org/10.1081/SCC-120013726.

(22) Lee, S.; Kim, J. N.; Kim, E.; Kim, M. S.; Lee, H. K. Biological Evaluation of Dilactone Lignan Analogues of Phellinsin a as Chitin Synthase II Inhibitors. *Bull. Korean Chem. Soc.* **2009**, *30* (12), 3092–3094. https://doi.org/10.5012/bkcs.2009.30.12.3092.

(23) Zheng, C.; Guo, Y.; Meng, Y.; Dou, S.; Shao, J.; Yang, Y. Synthesis of Salidroside Analogues and Their Ability of DPPH Radical Scavenging Activity. *Indian J. Chem. - Sect. B Org. Med. Chem.* **2013**, *52* (5), 654–664. https://doi.org/10.1002/chin.201338200.

(24) Okuda, K.; Oowatashi, R.; Yoshida, A.; Matsuo, Y.; Saito, Y. Stereoselectivity in Oxidative Dimerization of Catechins During Tea Fermentation. In *59th Symposium on the Chemistry of Natural Products*; Sapporo, Japan, 2017.

(25) de Toledo, R. A.; Santos, M. C.; Suffredini, H. B.; Homem-de-Mello, P.; Honorio, K. M.; Mazo, L. H. DFT and Electrochemical Studies on Nortriptyline Oxidation Sites. *J. Mol. Model.* **2009**, *15* (8), 945–952. https://doi.org/10.1007/s00894-009-0451-z.

(26) Riahi, S.; Norouzi, P.; Bayandori Moghaddam, A.; Ganjali, M. R.; Karimipour, G. R.; Sharghi, H. Theoretical and Experimental Report on the Determination of Oxidation Potentials of Dihydroxyanthracene and Thioxanthens Derivatives. *Chem. Phys.* **2007**, *337* (1–3), 33–38. https://doi.org/10.1016/j.chemphys.2007.06.018.

(27) Nagaraja, C.; Venkatesha, T. V. The Influence of Electron Donating Tendency on Electrochemical Oxidative Behavior of Hydroquinone: Experimental and Theoretical Investigations. *Electrochim. Acta* **2018**, *260*, 221–234. https://doi.org/10.1016/j.electacta.2017.12.035.

(28) Goto, H.; Osawa, E. Corner Flapping: A Simple and Fast Algorithm for Exhaustive Generation of Ring Conformations. *J. Am.* Chem*. Soc.* **1989**, *111* (24), 8950–8951. https://doi.org/10.1021/ja00206a046.

(29) Goto, H.; Osawa, E. An Efficient Algorithm for Searching Low-Energy Conformers of Cyclic and Acyclic Molecules. *J. Chem. Soc. Perkin Trans. 2* **1993**, *2* (2), 187–198. https://doi.org/10.1039/p29930000187.

(30) Frisch, M. J.; Trucks, G. W.; Schlegel, H. B.; Scuseria, G. E.; Robb, M. A.; Cheeseman, J. R.; Scalmani, G.; Barone, V.; Petersson, G. A.; Nakatsuji, H.; et al. Gaussian 2016. Gaussian Inc.: Wallingford, CT 2017.

(31) Chaquin, P. Absolute Electronegativity and Hardness: An Analogy with Classical Electrostatics Suggests an Interpretation of the Parr “electrophilicity Index” as a “Global

Energy Index" Leading to the "Minimum Electrophilicity Principle." *Chem. Phys. Lett.* **2008**, *458* (1–3), 231–234. https://doi.org/10.1016/j.cplett.2008.04.087.

(32) Luo, J.; Xue, Z. Q.; Liu, W. M.; Wu, J. L.; Yang, Z. Q. Koopmans' Theorem for Large Molecular Systems within Density Functional Theory. *J. Phys. Chem. A* **2006**, *110* (43), 12005–12009. https://doi.org/10.1021/jp063669m.

(33) Parr, R. G.; Szentpaly, L. v; Liu, S. Electrophilicity Index. *J. Am. Chem. Soc.* **1999**, *121* (9), 1922–1924. https://doi.org/10.1021/ja983494x.

(34) Kiyooka, S. I.; Kaneno, D.; Fujiyama, R. Intrinsic Reactivity Index as a Single Scale Directed toward Both Electrophilicity and Nucleophilicity Using Frontier Molecular Orbitals. *Tetrahedron* **2013**, *69* (21), 4247–4258. https://doi.org/10.1016/j.tet.2013.03.083.